Available online at www.sciencedirect.com
SCIENCE DIRECT®
Journal of Magnetic Resonance 165 (2003) 1–8
JMR Journal of Magnetic Resonance
www.elsevier.com/locate/jmr

Hydrogen bonds lengths in nucleic acids estimated from longitudinal nitrogen-15 relaxation

Dimitri Bytchenkoff and Geoffrey Bodenhausen*

Institut de Chimie Moléculaire et Biologique, Ecole Polytechnique Fédérale de Lausanne, BCH, 1015 Lausanne, Switzerland
Département de Chimie, associé au CNRS, Ecole Normale Supérieure, 24, rue Lhomond, 75231 Paris Cedex 05, France

Received 5 March 2003; revised 12 July 2003

Abstract

A new NMR method has been designed for the measurement of the longitudinal relaxation rates of both donor and acceptor nitrogen-15 nuclei in Watson–Crick base pairs in ^{15}N-enriched nucleic acids. The experiment was applied to a 22-nucleotide RNA hairpin. The lengths of four hydrogen bonds could be estimated from the longitudinal relaxation rates.

Keywords: Nucleic acids; Watson–Crick base pairs; Hydrogen bonds; Longitudinal nitrogen-15 relaxation

1. Introduction

Only intimate knowledge of both structure and dynamics of RNA's allows one to grasp the intriguing mechanisms that enable them to play their biological role. Nuclear spin relaxation measurements represent a versatile approach for studying both the average structure and structural fluctuations occurring on time scales from picoseconds to milliseconds. In this work, we present a new method for the measurement of the longitudinal relaxation times $R_1 = 1/T_1$ of both donor and acceptor nitrogen nuclei in Watson–Crick base pairs in ^{15}N-enriched nucleic acids. By supplementing measurements of donor nitrogen relaxation rates [1], information about acceptor nitrogen relaxation allows one to estimate the lengths of hydrogen bonds. The experiment was applied to the ^{15}N-enriched 22-nucleotide RNA hairpin GGCGAAGUCGAAAGAUGGCGCC [2] (see Fig. 1.) By determining the dipolar contributions to the longitudinal relaxation rates at two different static magnetic fields, one can estimate the lengths of the internucleotide hydrogen bonds for the four base pairs U8–A15, G2–C21, G20–C3, and G14–C9 of the RNA hairpin. These lengths can then be used as constraints in solving structures of nucleic acids.

2. Experimental

A Shigemi sample tube containing 2.2 mM RNA (see Fig. 1), 200 mM NaCl, 10 mM sodium phosphate, 0.1 mM EDTA, 90% H_2O, and 10% D_2O at pH 5.6 was investigated at 7 and 9.4 T (300 and 400 MHz) at 300 K using DMX-300 and DMX-400 NMR Bruker spectrometers equipped with triple-axis pulsed-field gradient TBI probes optimised for ^{1}H detection. Fig. 2 shows the pulse sequence that was developed to measure the longitudinal relaxation rates $R_1 = 1/T_1$ of the donor and acceptor nitrogen nuclei. A series of spectra were recorded with this sequence for relaxation delays $\tau_m = 3$, 100, 200, and 300 ms. Each data matrix comprised 64×512 complex data points with spectral widths of 20 and 100 ppm in ω_1 and ω_2, respectively; 192 scans per t_1 increment were recorded. The experiments were performed with the ^{1}H carrier positioned on the H_2O resonance and the ^{15}N carrier at 181.5 ppm. A gradient-tailored water suppression sequence [3] is used to attenuate the amplitude of the solvent signal. The programme nmrPipe was used for data processing [4]. A Monte Carlo error analysis was performed using the

* Corresponding author. Fax: +33-1-44-32-33-97.
E-mail address: Geoffrey.Bodenhausen@ens.fr (G. Bodenhausen).

1090-7807/$ - see front matter © 2003 Elsevier Inc. All rights reserved.
doi:10.1016/S1090-7807(03)00271-4

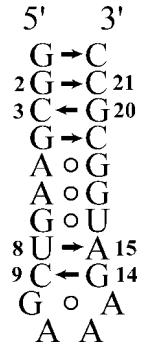

Fig. 1. Schematic structure of the 22-nucleotide RNA hairpin GGCG AAGUCGAAAGAUGGCGCC. Mismatched base pairs are represented by open circles. Matched base pairs are indicated by arrows from donor to acceptor. Only four imino protons (between numbered bases) can be observed in the proton spectrum, the others being broadened by exchange.

Matlab package, assuming a Gaussian error distribution [5].

The sequence of Fig. 2 begins by saturating the 'native' longitudinal nitrogen magnetisation by a $\pi/2$ pulse followed by a pulsed-field gradient. The sequence ends with WALTZ-16 decoupling applied to ^{15}N during data acquisition. Henceforth, the symbols N^D and N^A refer to the angular momentum operators of the donor and acceptor nitrogen nuclei. The sequence of coherence transfer steps starts with the conversion of the magnetisation of the imino proton H to N^D via the one-bond scalar coupling $^1J(HN^D)$ to create $2H_zN_y^D$ at point ***a***. This antiphase nitrogen coherence undergoes a transformation under the homonuclear scalar coupling $^{2h}J(N^DN^A)$ during the interval Δ. At the same time, the displacement of the two 180° proton pulses between ***a*** and ***b*** by $\tau/4$ from the middle of the $\Delta/2$ intervals allows the heteronuclear coupling $^1J(HN^D)$ to act on the coherence during an interval τ. The resulting coherences at point ***b*** are:

$$\sigma = -N_x^D \cos[\pi^{2h}J(N^DN^A)\Delta] - 2N_y^DN_z^A \times \sin[\pi^{2h}J(N^DN^A)\Delta] \quad (1)$$

The nitrogen $90°_x$ pulse between ***b*** and ***c*** leaves the in-phase coherence $-N_x^D$ unchanged while transforming the anti-phase coherence $-2N_y^DN_z^A$ into $2N_z^DN_y^A$ at point ***c***. To cancel effects of cross-correlated CSA/DD relaxation, two proton inversion pulses were applied between points ***c*** and ***d***, one between points ***e*** and ***f***, and two between points ***f*** and ***g*** in Fig. 2. The coherences are allowed to transform under the scalar coupling $^{2h}J(N^DN^A)$ during the second interval Δ so as to create the following product operators at point ***d***

$$\begin{aligned}\sigma = & -N_x^D \cos^2[\pi^{2h}J(N^DN^A)\Delta] - 2N_y^DN_z^A \\ & \times \cos[\pi^{2h}J(N^DN^A)\Delta]\sin[\pi^{2h}J(N^DN^A)\Delta] \\ & + 2N_z^DN_y^A \sin[\pi^{2h}J(N^DN^A)\Delta]\cos[\pi^{2h}J(N^DN^A)\Delta] \\ & - N_x^A \sin^2[\pi^{2h}J(N^DN^A)\Delta]. \end{aligned} \quad (2)$$

The $90°_y$ nitrogen pulse at point ***d*** transforms these product operators into:

$$\begin{aligned}\sigma = & N_z^D \cos^2[\pi^{2h}J(N^DN^A)\Delta] - 2N_y^DN_x^A \\ & \times \cos[\pi^{2h}J(N^DN^A)\Delta]\sin[\pi^{2h}J(N^DN^A)\Delta] \\ & + 2N_x^DN_y^A \sin[\pi^{2h}J(N^DN^A)\Delta]\cos[\pi^{2h}J(N^DN^A)\Delta] \\ & + N_z^A \sin^2[\pi^{2h}J(N^DN^A)\Delta]. \end{aligned} \quad (3)$$

The sum of the second and third of these product operators represents pure zero-quantum coherence:

$$2N_x^DN_y^A - 2N_y^DN_x^A = i(N_+^DN_-^A - N_-^DN_+^A) = \{ZQC\}. \quad (4)$$

Unless specific precautions are taken to suppress this zero-quantum coherence, it may precess during the relaxation period τ_m, be transferred into $2N_z^DN_y^A$ and $-2N_y^DN_z^A$ at point ***f*** , be labelled with N^D and N^A frequencies, respectively, during the evolution time t_1, and

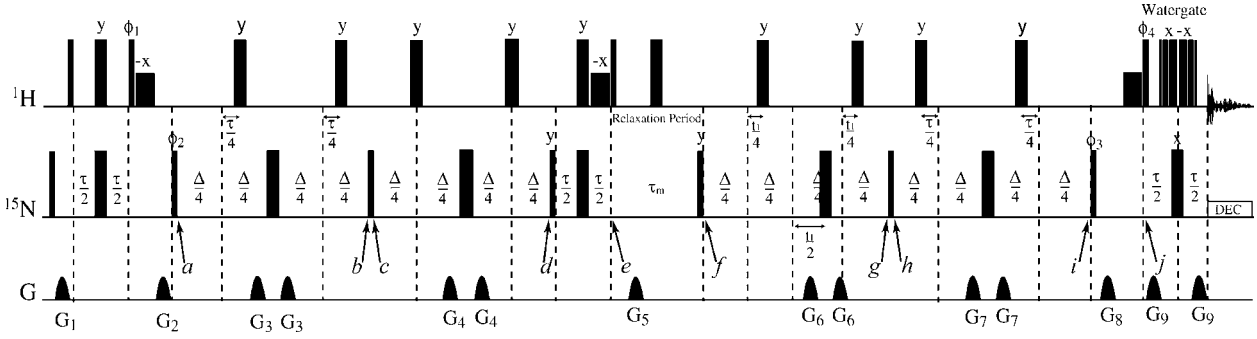

Fig. 2. Experimental scheme for the simultaneous measurement of the longitudinal relaxation rates $R_1 = 1/T_1$ of both the $^{15}N^D$ donor and $^{15}N^A$ acceptor nuclei in hydrogen bonded systems N^D–H $\cdots$ N^A in nucleic acids. Narrow and wide rectangles represent 90° and 180° pulses, respectively. The delays $\tau = 5.6$ ms $\approx 1/[2^1J(N^DH)]$ and $\Delta = 44$ ms $\approx 1/[4^{2h}J(N^DN^A)]$. Selective rectangular 90° pulses of 0.91 ms duration were applied three times in the sequence to flip the water magnetisation back to the $+z$-axis. Unless otherwise indicated the phases of the pulses are along the x-axis. The phase cycling was $\phi_1 = 16(y,-y)$; $\phi_2 = 4(x,x,-x,-x)$; $\phi_3 = 8(x),8(-x)$, $\phi_4 = 4(x),4(-x),4(x),4(-x)$; $\phi_{receiver} = x,-x,-x,x,-x,x,x,-x,-x,x,x,-x,x,-x,-x,x$. Quadrature detection was achieved in the t_1 dimension by incrementing the phase of the 90° nitrogen pulse just before point ***f*** in States-TPPI manner. A gradient-tailored water suppression technique [3] was used with a pulse interval of 240 μs to optimise refocusing of the imino protons centred at 12.5 ppm. DEC refers to nitrogen decoupling.

be converted into observable ^{1}H magnetisation. To avoid this, the zero-quantum coherence was allowed to transform into $(4H_zN_x^DN_x^A + 4H_zN_y^DN_y^A)$ under the scalar coupling $^1J(HN^D)$ during the interval τ between points ***d*** and ***e***. Meanwhile the first and fourth terms of Eq. (3) were inverted by the 180° nitrogen pulse in the middle of this interval τ. After applying the 90° proton pulse, the product operators at point ***e*** are:

$$\begin{aligned}\sigma = &-N_z^D\cos^2[\pi^{2h}J(N^DN^A)\Delta] - 4H_yN_x^DN_x^A\\ &\times\cos[\pi^{2h}J(N^DN^A)\Delta]\sin[\pi^{2h}J(N^DN^A)\Delta]\\ &-4H_yN_y^DN_y^A\sin[\pi^{2h}J(N^DN^A)\Delta]\\ &\times\cos[^{2h}J(N^DN^A)\Delta] - N_z^A\sin^2[\pi^{2h}J(N^DN^A)\Delta]. \quad (5)\end{aligned}$$

The sum of the second and third of these product operators represents three-spin single-quantum coherence:

$$\begin{aligned}&-4H_yN_x^DN_x^A + 4H_yN_y^DN_y^A = 2i[H_+N_+^DN_-^A\\ &+H_+N_-^DN_+^A + H_-N_+^DN_-^A + H_-N_-^DN_+^A], \quad (6)\end{aligned}$$

which can be dephased by applying a pulsed-field gradient G_5. This procedure will be referred to as 'zero-quantum elimination.'

An alternative that has been explored is the application at point ***d*** of a selective sine-modulated nitrogen E-BURP pulse [6], which rotates N_z^D and N_z^A by $(90°)_{+y}$ and $(90°)_{-y}$, respectively, thus leading to a transformation of the product operators of Eq. (2) into

$$\begin{aligned}\sigma = &N_z^D\cos^2[\pi^{2h}J(N^DN^A)\Delta] + 2N_y^DN_x^A\\ &\times\cos[\pi^{2h}J(N^DN^A)\Delta]\sin[\pi^{2h}J(N^DN^A)\Delta]\\ &+2N_x^DN_y^A\sin[\pi^{2h}J(N^DN^A)\Delta]\cos[\pi^{2h}J(N^DN^A)\Delta]\\ &-N_z^A\sin^2[\pi^{2h}J(N^DN^A)\Delta] \quad (7)\end{aligned}$$

In this case, the interval τ between ***d*** and ***e*** may be dropped. The sum of the second and third of these product operators represents pure double-quantum coherence:

$$2N_y^DN_x^A + 2N_x^DN_y^A = i(N_-^DN_-^A - N_+^DN_+^A) = \{DQC\} \quad (8)$$

which can be dephased by the pulsed-field gradient G_5. If the selective rotations were ideal, the zero-quantum coherence would vanish. However, the E-BURP pulse only gives the desired excitation profile if the flip angle is properly calibrated and if the nutation occurs precisely about the $+y$ and $-y$-axes of the rotating frames of the donor and acceptor nuclei. The calibration of a modulated E-BURP pulse for the two nitrogen nuclei represents a time-consuming task. This is why the elimination of zero-quantum coherence appears preferable to the sine-modulated E-BURP.

The longitudinal magnetisations N_z^D and N_z^A, represented by the first and fourth product operators in Eq. (5), undergo partial spin-lattice relaxation during the delay τ_m. We consider a form of difference spectroscopy where the signals are derived in alternation from $+N_z^{D/A}$ and $-N_z^{D/A}$, which can be achieved by alternating the phase ϕ_1 in Fig. 2. If one considers the difference between the resulting signals, longitudinal relaxation leads to a mono-exponential decay to zero. The normalised difference between the density operators of the two complementary experiments can be written as:

$$\begin{aligned}\Delta\sigma = &-N_z^D\cos^2[\pi^{2h}J(N^DN^A)\Delta]\exp(-\tau_m/T_1^D)\\ &-N_z^A\sin^2[\pi^{2h}J(N^DN^A)\Delta]\exp(-\tau_m/T_1^A), \quad (9)\end{aligned}$$

where T_1^D and T_1^A stand for the longitudinal relaxation times of the donor and acceptor nitrogen nuclei, respectively.

At point ***f***, a nitrogen $90°_y$ pulse rotates the remainder of the longitudinal magnetisations back onto the transverse plane to give

$$\begin{aligned}\Delta\sigma = &-N_x^D\cos^2[\pi^{2h}J(N^DN^A)\Delta]\exp(-\tau_m/T_1^D)\\ &-N_x^A\sin^2[\pi^{2h}J(N^DN^A)\Delta]\exp(-\tau_m/T_1^A). \quad (10)\end{aligned}$$

Henceforth, we shall limit our attention to the fate of the coherences of interest. The following two nitrogen 180° pulses are shifted from the centres of the next Δ delays in order to achieve a constant-time labelling of transverse magnetisation of both $^{15}N^D$ and $^{15}N^A$ nuclei by their corresponding chemical shifts $\Omega(N^D)$ and $\Omega(N^A)$. Furthermore the magnetisations are effected by the coupling $^{2h}J(N^DN^A)$ during the third Δ interval between points **f** and **g**. The resulting terms are

$$\begin{aligned}\Delta\sigma = &-N_x^D\cos^3[\pi^{2h}J(N^DN^A)\Delta]\cos[\Omega(N^D)t_1]\\ &\times\exp(-\tau_m/T_1^D) - 2N_z^DN_y^A\sin^3[\pi^{2h}J(N^DN^A)\Delta]\\ &\times\cos[\Omega(N^A)t_1]\exp(-\tau_m/T_1^A) \quad (11)\end{aligned}$$

at point ***g***. The nitrogen $90°_x$ pulse between ***g*** and ***h*** leaves the first coherence unchanged while transforming $-2N_z^DN_y^A$ into $2N_y^DN_z^A$ at point ***h***. Then the coherences are permitted to undergo a transformation under the coupling $^{2h}J(N^DN^A)$ during the fourth interval Δ between points ***h*** and ***i*** as well as under the coupling $^1J(HN^D)$ during τ. This results in the creation of a state

$$\begin{aligned}\Delta\sigma = &-2H_zN_y^D\cos^4[\pi^{2h}J(N^DN^A)\Delta]\cos[\Omega(N^D)t_1]\\ &\times\exp(-\tau_m/T_1^D) - 2H_zN_y^D\sin^4[\pi^{2h}J(N^DN^A)\Delta]\\ &\times\cos[\Omega(N^A)t_1]\exp(-\tau_m/T_1^A) \quad (12)\end{aligned}$$

at point ***i***. The last nitrogen and proton 90° pulses are applied in order to create

$$\begin{aligned}\Delta\sigma = &2H_yN_z^D\cos^4[\pi^{2h}J(N^DN^A)\Delta]\cos[\Omega(N^D)t_1]\\ &\times\exp(-\tau_m/T_1^D) + 2H_yN_z^D\sin^4[\pi^{2h}J(N^DN^A)\Delta]\\ &\times\cos[\Omega(N^A)t_1]\exp(-\tau_m/T_1^A) \quad (13)\end{aligned}$$

at point ***j***. These antiphase coherences are converted into observable magnetisation through the one-bond scalar coupling $^1J(HN^D)$ to create

$$\Delta\sigma = -\mathrm{H}_x \cos^4[\pi^{2h} J(\mathrm{N^D N^A})\Delta] \cos[\Omega(\mathrm{N^D})t_1] \times \exp(-\tau_\mathrm{m}/T_1^\mathrm{D}) - \mathrm{H}_x \sin^4[\pi^{2h} J(\mathrm{N^D N^A})\Delta] \times \cos[\Omega(\mathrm{N^A})t_1] \exp(-\tau_\mathrm{m}/T_1^\mathrm{A}). \quad (14)$$

The proton signal is recorded and Fourier transformed to give peaks with amplitudes that are proportional to $\Delta M_z^\mathrm{D}(\tau_\mathrm{m})$ and $\Delta M_z^\mathrm{A}(\tau_\mathrm{m})$:

$$\Delta M_z^{\mathrm{D/A}}(\tau_\mathrm{m}) = \Delta M_z^{\mathrm{D/A}}(\tau_\mathrm{m}=0)\exp(-\tau_\mathrm{m}/T_1^{\mathrm{D/A}}) \quad (15)$$

where $\Delta M_z^{\mathrm{D/A}}(\tau_\mathrm{m}) = M_z^{\mathrm{D/A}}(\tau_\mathrm{m}) - M_{z,\mathrm{eq}}^{\mathrm{D/A}}$, and where $M_{z,\mathrm{eq}}^{\mathrm{D/A}}$ is the equilibrium magnetisation, and $M_z^{\mathrm{D/A}}(\tau_\mathrm{m})$ the magnetisation remaining at the end of the relaxation delay τ_m. When the experiment is repeated for different values of τ_m the longitudinal relaxation rates $R_1^{\mathrm{D/A}} = 1/T_1^{\mathrm{D/A}}$ can be determined in the usual way.

3. Results and discussion

Fig. 3 shows $\Delta M_z^{\mathrm{D/A}}$ as a function of the relaxation period τ_m, normalised so that $\Delta M_z^{\mathrm{D/A}}(\tau_\mathrm{m}=0) = 1$. The longitudinal relaxation rates determined from these measurements are presented in Table 1.

The longitudinal relaxation of nitrogen nuclei in RNA is driven by CSA and dipolar interactions with neighbouring nuclei:

$$R_1^\mathrm{tot} = R_1^\mathrm{CSA} + \sum R_1^\mathrm{DD}(\mathrm{H}_i). \quad (16)$$

The CSA rates are

$$R_1^\mathrm{CSA} = d^\mathrm{CSA} J^{ij}(\omega_\mathrm{N}) \quad (17)$$

with $d^\mathrm{CSA} = (1/3)(\Delta\sigma_\mathrm{N})^2 \gamma_\mathrm{N}^2 B_\mathrm{o}^2$, where $\Delta\sigma_\mathrm{N} = \sigma_| - \sigma_\perp$ is the anisotropy of the nitrogen nuclear shielding tensor assumed to have cylindrical symmetry and γ_N the nitrogen-15 gyromagnetic ratio.

The spectral densities $J^{ij}(\omega_\mathrm{N})$ may show slight variations for different base pairs ij with local correlation times τ_c^{ij} of rotational diffusion, which is supposed to be isotropic:

$$J^{ij}(\omega) = (2/5)\tau_\mathrm{c}^{ij}/(1+\omega^2(\tau_\mathrm{c}^{ij})^2).$$

The dipolar rates are

$$R_1^\mathrm{DD}(\mathrm{H}_i) = (1/4)d^\mathrm{DD}(\mathrm{H}_i)\{3J^{ij}(\omega_\mathrm{N}) + J^{ij}(\omega_\mathrm{H}-\omega_\mathrm{N}) + 6J^{ij}(\omega_\mathrm{H}+\omega_\mathrm{N})\}. \quad (18)$$

$$R_1^\mathrm{DD}(\mathrm{H}_i) \approx (3/4)d^\mathrm{DD}(\mathrm{H}_i)J^{ij}(\omega_\mathrm{N}) \quad (19)$$

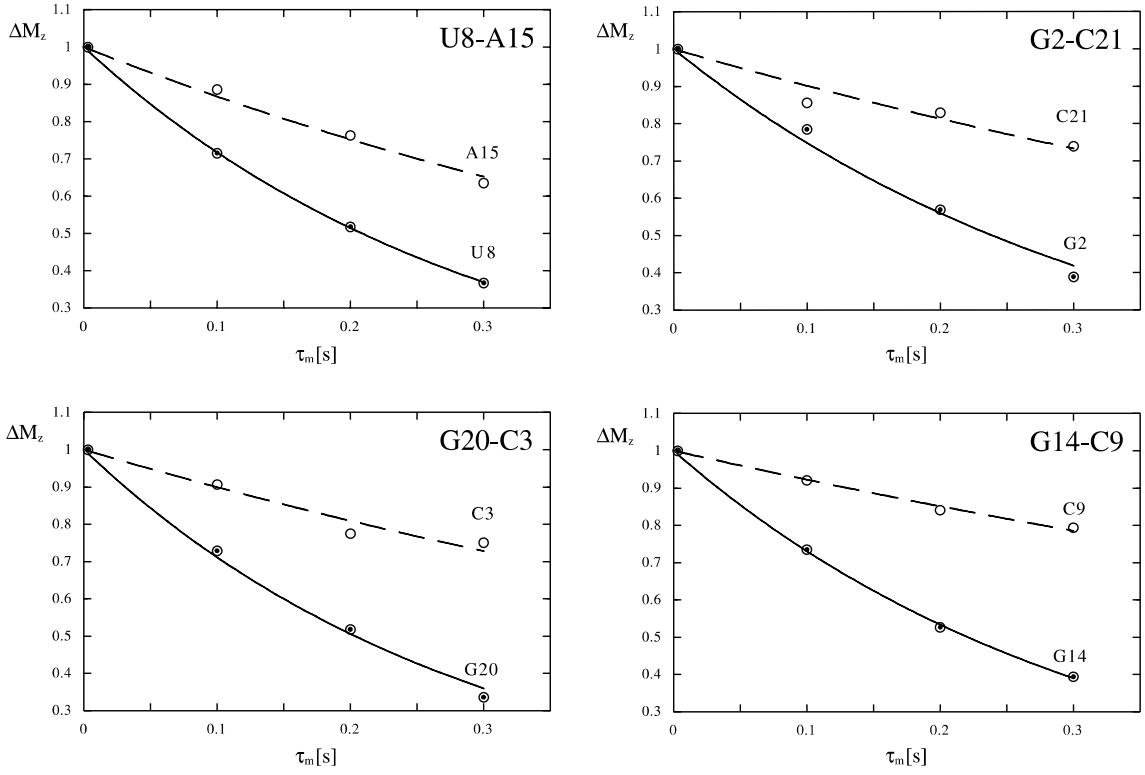

Fig. 3. Decay of the deviation of longitudinal magnetisation components $\Delta M_z^{\mathrm{D/A}} = M_z^{\mathrm{D/A}} - M_{z,\mathrm{eq}}^{\mathrm{D/A}}$ measured at 7 T and 300 K for τ_m = 3, 100, 200, and 300 ms for the base pairs U8–A15, G2–C21, G20–C3, and G14–C9 of the 22-nucleotide RNA hairpin of Fig. 1. The slowly relaxing responses correspond to the acceptor nitrogens $\mathrm{N^A}$ of adenines and cytosines, while the rapidly relaxing components correspond to the donor nitrogens $\mathrm{N^D}$ of uracils and guanines.

Table 1
Experimental longitudinal relaxation rates $R_1 = 1/T_1$ of the donor N^D and acceptor N^A nitrogen-15 nuclei for the base pairs U8–A15, G2–C21, G20–C3, G14–C9 of the 22-nucleotide RNA hairpin of Fig. 1 measured at static magnetic fields $B_o = 7$ and 9.4 T and a temperature of 300 K.

Base pair		$R_1 = 1/T_1(s^{-1})$	
Donor N^D	Acceptor N^A	7 T	9.4 T
U8		3.32 ± 0.15	2.71 ± 0.15
	A15	1.42 ± 0.06	1.94 ± 0.09
G2		2.90 ± 0.18	2.37 ± 0.17
	C21	1.04 ± 0.06	1.39 ± 0.08
G20		3.41 ± 0.13	2.84 ± 0.14
	C3	1.06 ± 0.04	1.41 ± 0.08
G14		3.14 ± 0.09	2.57 ± 0.10
	C9	0.81 ± 0.02	1.06 ± 0.04

Errors were estimated with a Monte-Carlo procedure [5].

with $d^{DD}(H_i) = (\mu_0/4\pi)^2\hbar^2\gamma_N^2\gamma_H^2[r(NH_i)]^{-6}$, where $r(NH_i)$ is the distance between either N^D or N^A and a proton H_i, τ_c^{ij} the local correlation time as defined above. The simplification in Eq. (19) obtained by retaining only the $J^{ij}(\omega_N)$ term is legitimate for a slowly tumbling macromolecule.

Using an estimate of the average correlation time of 3.5 ns [2] and experimentally determined ^{15}N chemical shift tensors of nucleic acids reported previously [7], one can estimate the CSA contributions to the relaxation of the donor nitrogen nuclei. At 7 T, these contributions are 0.11 s^{-1} for uracil and 0.14 s^{-1} for guanine, and they increase to 0.14 and 0.19 s^{-1} at 9.4 T. Therefore, comparing with the total relaxation rates of Table 1, the estimated CSA contributions amount to 3.3, 4.8, 4.1, 4.5% for the donor nitrogen nuclei of U8, G2, G20 and G14 at 7 T, and to 5.2, 8.0, 6.7, 7.4% of these rates at 9.4 T. Since this only leads to minor corrections to the calculations that follow, we believe that it is better to neglect the CSA contributions to the donor nitrogen relaxation rates, lest our prescriptions become needlessly complicated.

For the donor nitrogen nuclei N^D, we thus assume that relaxation is predominantly due to the neighbouring imino protons [7]. From the ratios $R_1^{DD}(B_o^I)/R_1^{DD}(B_o^{II})$ of the donor nitrogens at two different magnetic fields, one can estimate the local correlation times. In Table 1, $B_o^I = 7$ T, or 300 MHz for protons, and $B_o^{II} = 9.4$ T or 400 MHz. We may conclude that the local correlation times τ_c^{ij} lie between 3.0 and 3.3 ns (see Table 2). The variations in these local correlation times may be due to a combination of rotational anisotropy and fast local motions. If we had used dipolar rates of the donor nitrogen nuclei that were corrected by subtracting the estimated CSA rates from the total relaxation rates, their ratios would have yielded local correlation times of 3.5, 3.6, 3.4, 3.6 ns for U8, G2, G20 and G14, respectively, instead of the values given in Table 2. Adjusting the correlation times in this manner would lead to marginal changes in the estimates of the distances $r(N^D\text{–}H)$ and $r(H\cdots N^A)$ discussed below.

Table 2
Local rotational correlation times τ_c^{ij} determined from the ratios $R_1^{DD}(B_o^I)/R_1^{DD}(B_o^{II})$ of the *donor* nitrogen nuclei measured at two different magnetic fields $B_o^I = 7$ T and $B_o^{II} = 9.4$ T, assuming that their relaxation is predominantly driven by dipolar interactions with the neighbouring imino protons.

Base pair ($N^D \rightarrow N^A$)	(i,j)	τ_c^{ij} (ns)	$r(N^D\text{–}H)$ (Å)
U8 → A15	(8,15)	3.3 ± 1.3	1.05 ± 0.03
G2 → C21	(2,21)	3.2 ± 1.8	1.07 ± 0.04
G20 → C3	(20,3)	3.0 ± 1.1	1.04 ± 0.03
G14 → C9	(14,9)	3.2 ± 0.8	1.06 ± 0.02

The local correlation times τ_c^{ij} are assumed to be common to both donor and acceptor nucleotides in each base pair (i,j). The distances $r(N^D\text{–}H)$ were calculated using the local correlation times τ_c^{ij}. They may be compared with the estimate used by Rüdisser and Tinoco of $r(N^D\text{–}H) = 1.01$ Å for all base pairs.

Using Eq. (19) and the local correlation times τ_c^{ij}, the distances $r(N^D\text{–}H)$ between the donor nitrogen nuclei and neighbouring imino protons can be estimated to lie between 1.04 and 1.07 Å (Table 2), which is a bit longer than the average distance $r(N^D\text{–}H) = 1.01$ Å that was assumed in the structure determined by Rüdisser and Tinoco [2].

It is clear from Eqs. (16)–(18) that the contributions R_1^{CSA} and R_1^{DD} to the total longitudinal relaxation rates R_1^{tot} of the acceptor nitrogen nuclei can be discriminated provided that the latter are measured at two different static magnetic fields. According to Eqs. (16)–(18) and using the local rotational correlation times τ_c^{ij}, the dipolar relaxation rate at B_o^I can be determined as follows:

$$R_1^{DD}(B_o^I) = (k_{ij}^{CSA}R_1^{tot}(B_o^I) - R_1^{tot}(B_o^{II}))/(k_{ij}^{CSA} - k_{ij}^{DD}) \tag{20}$$

where k_{ij}^{CSA} and k_{ij}^{DD} (Table 3) stand for the ratios

$$k_{ij}^{CSA} = R_1^{CSA}(B_o^I)/R_1^{CSA}(B_o^{II}) = (B_o^I/B_o^{II})^2 J^{ij}(\omega_N^I)/J^{ij}(\omega_N^{II}) \tag{21}$$

and

$$k_{ij}^{DD} = R_1^{DD}(B_o^I)/R_1^{DD}(B_o^{II}) = [3J^{ij}(\omega_N^I) + J^{ij}(\omega_H^I - \omega_N^I) + 6J^{ij}(\omega_H^I + \omega_N^I)] \times [3J^{ij}(\omega_N^{II}) + J^{ij}(\omega_H^{II} - \omega_N^{II}) + 6J^{ij}(\omega_H^{II} + \omega_{Nu}^{II})]^{-1} \tag{22}$$

Table 3
Ratios k_{ij}^{CSA} and k_{ij}^{DD} of Eqs. (21) and (22) for $B_o^I = 7$ T and $B_o^{II} = 9.4$ T, estimated from the averages of the local correlation times τ_c^{ij} of Table 2

Base pair ($N^D \rightarrow N^A$)	(i,j)	k_{ij}^{CSA}(acceptor)	k_{ij}^{DD}(acceptor)
U8 → A15	(8,15)	1.47	0.81
G2 → C21	(2,21)	1.47	0.81
G20 → C3	(20,3)	1.49	0.82
G14 → C9	(14,9)	1.47	0.81

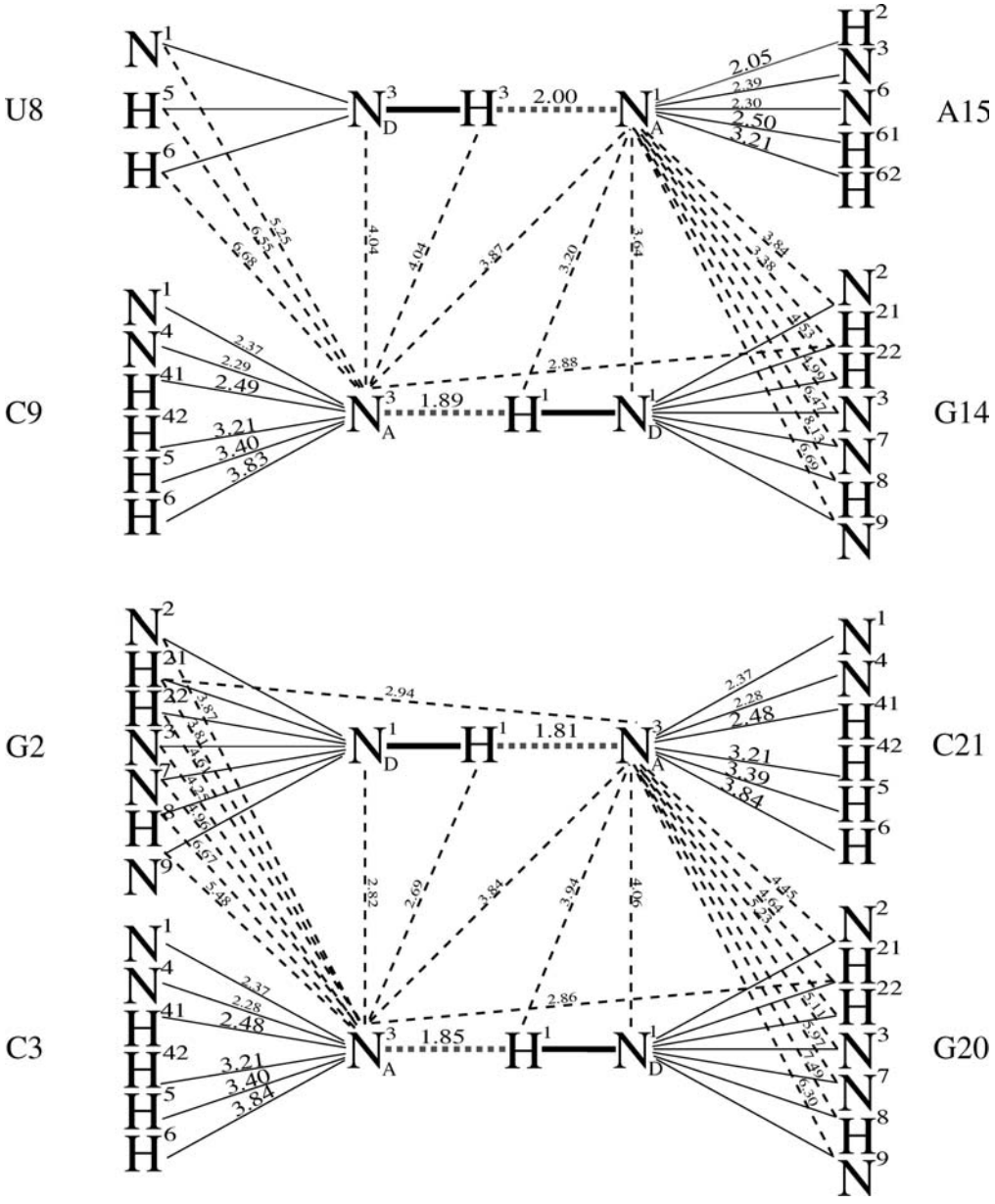

Fig. 4. Distances (in Å) between neighbouring nuclei in the base pairs U8–A15 and G14–C9 (top), and G2–C21 and G20–C3 (below) of the 22-nucleotide RNA hairpin of Fig. 1 calculated from the NMR structure determined by Rüdisser and Tinoco [2]. Short distances between nuclei with large gyromagnetic ratios, which lead to significant dipolar relaxation, are emphasized by using larger fonts.

The distances between the neighbouring nuclei are shown in Fig. 4 for the base pairs U8–A15 and G14–C9 (top), and for the base pairs G2–C21 and G20–C3 (below). These internuclear distances were derived from the structure obtained by NMR by Rüdisser and Tinoco [2]. For the acceptor nitrogen nucleus N_A^1 of A15, apart from the nearby imino proton H^3 of U8, there are only three other protons H^2, H^{61}, and H^{62} that can make significant contributions to the dipolar relaxation. For the acceptor nitrogen nucleus N_A^3 of the nucleotides C9, C21, C3 the dipolar relaxation is mainly due to the nearby imino proton H^1 and to four other protons H^{41}, H^{42}, H^5, and H^6. The contributions from remote protons were calculated using Eq. (18) (Table 4). Subtracting these remote dipolar rates from the total dipolar rates calculated from Eq. (20) yields the rates due to the neighbouring imino protons (Table 5). These rates allow one to estimate the hydrogen bond lengths $r(\mathrm{H}\cdots\mathrm{N^A})$ (Table 5).

In addition to the protons belonging to the same or to the opposite base, there are a limited number of more distant protons that belong to adjacent nucleotides and that may also contribute to the dipolar relaxation of the acceptor nitrogen nuclei (see Fig. 4). In particular, the nuclei H^1 and H^{21} of G14 are situated at distances shorter than 4 Å from the acceptor nitrogen nucleus N_1^A

Table 4
Calculated remote contributions (all rates in s^{-1}) to the dipolar relaxation rates $R_1^{DD} = 1/T_1^{DD}$ at $B_o = 7\,T$ (300 MHz) of the acceptor N^A nitrogen-15 nuclei in adenine and cytosine in the base pairs U8–A15, G2–C21, G20–C3, G14–C9 of the 22-nucleotide RNA hairpin of Fig. 1 using the distances $r(N^A - H_i)$ shown with large fonts in Fig. 4 and the local correlation times τ_c^{ij} of Table 2

Nucleotide (acceptor)	$R1^{DD}(N^1–H^2)$	$R1^{DD}(N^1–H^{61})$	$R1^{DD}(N^1–H^{62})$	
A15	0.0609	0.0184	0.0040	
Nucleotide (acceptor)	$R1^{DD}(N^3–H^{41})$	$R1^{DD}(N^3–H^{42})$	$R1^{DD}(N^3–H^5)$	$R1^{DD}(N^3–H^6)$
C21	0.0192	0.0041	0.0029	0.0014
C3	0.0190	0.0041	0.0029	0.0014
C9	0.0189	0.0041	0.0029	0.0014

Table 5
Estimated $R_1^{CSA}(N^A)$ and $R_1^{DD}(N^A)$ contributions of Eq. (20) to the total relaxation rate $R_1^{tot}(N^A)$ at 7 T of Table 1; sum of the contributions $\sum R_1^{DD}(N^A–H^i)$ due to nearby non-imino protons; estimated contributions due to the nearby imino protons $R_1^{DD}(H^i \cdots N^A)$, and internucleotide hydrogen bond lengths estimated in this work as well as those determined previously [2]

Base pair	$R_1^{CSA}(N^A)$ (s^{-1})	$R_1^{DD}(N^A)$ (s^{-1}) (all protons)	$\sum R_1^{DD}(N^A–H^i)$ (s^{-1}) (remote protons only)	R_1^{DD} ($H \ldots N^A$) (s^{-1}) (imino protons only)	$r(H \ldots N^A)$ (Å)	
					This work	Reference [2]
U8–A15	1.21	0.21	0.08	0.13	1.80 ± 0.44	2.00
G2–C21	0.83	0.21	0.03	0.18	1.71 ± 0.29	1.81
G20–C3	0.80	0.26	0.03	0.23	1.63 ± 0.17	1.85
G14–C9	0.61	0.20	0.03	0.17	1.72 ± 0.13	1.89

of A15. The nuclei H^{21} of G14 and G2 are also located at distances shorter than 3 Å from the acceptor nitrogen N_3^A nuclei of C9 and C21, respectively. So are H^{21} of G20 and H^1 of C21 with respect to the acceptor nitrogen nucleus N_3^A of C3 (see Fig. 4). The resulting dipolar contributions are however small compared to those due to the imino protons. The distances between an acceptor nitrogen nucleus and remote protons belonging to the opposite base or to adjacent bases along the same strand, which were determined by NMR [2], are obviously less well known than distances to protons belonging to the same base. That is why we did not take any remote protons into consideration, neither those on opposite bases nor those on adjacent bases. This may lead slightly to overestimate the dipolar relaxation rates caused by neighbouring imino protons, and hence slightly to underestimate the lengths of the hydrogen bonds.

4. Conclusions

A new NMR method allows one to measure the longitudinal relaxation rates of both donor and acceptor nitrogen nuclei in Watson–Crick base pairs in ^{15}N-enriched nucleic acids. Assuming that the relaxation rates of the donor nitrogen nuclei are largely dominated by dipolar interactions to the neighbouring imino protons, the local correlation times τ_c^{ij} can be determined using the ratios of the relaxation rates measured at two different fields. These correlation times τ_c^{ij} have been found to be slightly shorter than those reported previously [2]. The distances $r(N^D–H)$ between the donor nitrogen nuclei and the imino protons calculated using the local correlation times τ_c^{ij} appear reasonable. By separating contributions to the overall relaxation rates from the acceptor nitrogen chemical shift anisotropy and from other protons on the same base, one obtains estimates of the dipolar interactions between the acceptor nitrogens and the imino protons. This allows one to estimate the lengths of the hydrogen bonds. In the RNA fragment of the Fig. 1, the lengths of the hydrogen bonds were found to be in reasonable agreement with those reported previously [2]. If the relaxation rates were measured at lower magnetic fields, the errors of the hydrogen bond lengths could be reduced. The main limitation of the experimental scheme arises from the small $J(N^DN^A)$ couplings. For larger nucleic acids, one may need to resort to higher magnetic fields to increase the dispersion of the chemical shifts and the sensitivity. However, as the molecular mass of the nucleic acid increases, the efficiency of coherence transfer between donor and acceptor nitrogen nuclei will be attenuated because the T_2's are shorter. At the same time, the increasing CSA contribution to the relaxation of the acceptor nitrogen nuclei will tend to mask the dipolar rates, which would lead to poorer accuracy in the determination of hydrogen bond lengths.

Acknowledgments

We are indebted to Dr. Simon Rüdisser (Novartis) for the synthesis of the RNA sample. This work was supported by the Fonds National de la Recherche Scientifique (FNRS) and the Commission pour la Technologie

et l'Innovation (CTI) of Switzerland, and by the Centre National de la Recherche Scientifique (CNRS) of France.

References

[1] M. Akke, R. Fiala, F. Jiang, D. Patel, A.G. Palmer III, RNA 3 (1997) 702–709.
[2] S. Rüdisser, I. Tinoco Jr., J. Mol. Biol. 295 (2000) 1211–1223.
[3] V. Sklenár, M. Piotto, R. Leppik, V. Saudek, J. Magn. Reson., Series A 102 (1993) 241–245.
[4] F. Delaglio, S. Grzesiek, G.W. Vuister, G. Zhu, J. Pfeifer, A. Bax, J. Biomol. NMR 6 (1995) 277–293.
[5] P.R. Bevington, D.K. Robinson, Data Reduction and Error Analysis for the Physical Sciences, McGraw-Hill Inc, New York, 1992.
[6] H. Geen, R. Freeman, J. Magn. Reson 93 (1991) 93–141.
[7] J.Z. Hu, J.C. Facelli, D.W. Alderman, R.J. Pugmire, D.M. Grant, J. Am. Chem. Soc. 120 (1998) 9863–9869.